Atomic and electronic structures of oxygen-adsorbed Si(001) surfaces

Toshihiro Uchiyama
Matsushita Research Institute Tokyo, Inc., 3-10-1 Higashi-mita, Tama-ku, Kawasaki 214, Japan

Masaru Tsukada
Department of Physics, University of Tokyo, 7-3-1 Hongo, Bunkyo-ku, Tokyo 113, Japan
(Received 20 September 1995)

We investigate the stable structures of oxygen-adsorbed Si(001) surfaces and their electronic states. For this study, the first-principles molecular-dynamics method with the ultrasoft pseudopotential scheme is applied. The oxygen and silicon atoms are fully relaxed according to the calculated atomic forces for the optimized geometries. We find three (meta)stable sites for atomic oxygen adsorption: a dimer-bridge site and two different backbond sites of the dimer atoms. The original dimer bond is decomposed, or preserved and twisted, respectively. Most energetically favorable is the backbond site of the down dimer atom. Here, the electronegativity of oxygen enhances the ionicity of the dimer bond. Further, we simulate scanning tunneling microscopy images of the oxygen-adsorbed surfaces. The features of the most stable geometry are in good agreement with the observed ones.

I. INTRODUCTION

Atomically controlled oxidation of silicon surfaces is an eagerly desired technique in semiconductor device technology. It is indispensable to the realization of oxide layers with an atomic flatness and thickness. The practical oxidation reaction includes various elementary processes such as dissociation, adsorption, and diffusion of O_2 molecules through the surface, and bond formations between Si and O atoms near the surface or the interface. However, the microscopic phenomena and mechanism in those processes have been poorly understood so far. In this work, we concentrate on the initial stage of the oxidation on the Si(001) surface, especially on the atomic oxygen adsorption.

Until now, many experimental and theoretical works have been devoted to reveal atomic and electronic structures of the oxide complexes.[1] For example, Schaefer *et al.*[2] and Incoccia *et al.*[3] have reported that Si-O-Si complexes exist at the early stage of the oxidation in high-resolution electron-energy-loss spectroscopy (HREELS) and surface-extended x-ray-adsorption fine-structure (SEXAFS) measurement, respectively. In the HREELS, it is inferred that the oxygen atom is inserted into the Si-Si backbond. In the SEXAFS, it is discussed that the oxygen atom occupies two different bridge positions. Here, the Si-O bond length is reported to be 1.65 Å and the Si-O-Si bond angle to be about 130° or 120°.

Recently, scanning tunneling microscopy (STM) has been utilized to study the microscopic phenomena due to oxidation at room temperature.[4–6] STM is one of the most powerful tools for observing local atomic structures on the surface. In these experiments, bright spots appear irrelevantly to the bias polarity of the tip. However, the observed features such as position, height, and thermal stability are different in the experiments. Avouris and Cahill[5] have identified these bumps as isolated dimers made of Si atoms ejected from the surface. Kliese *et al.*[4] have insisted that they are weakly bound species of oxygen atoms or molecules. In addition, Kliese *et al.* have found small protrusions in the filled-states images at the very early stage of the oxidation. These spots appear most frequently in a bridging position between dimer rows with a height of about 0.2 Å. It is intriguing that they induce local dimer buckling.

Theoretically, Miyamoto and co-workers[7] have investigated the oxygen-adsorbed structures by applying the first-principles total-energy and force calculations. They have found three (meta)stable sites for the adsorption. The most stable geometry is that the oxygen atom is inserted into the dimer bond, i.e., the adsorption to the dimer-bridge (DB) site. Metastable are the on-dimer and the backbond (BB) site. Here, the original dimer is preserved or twisted, respectively. For both of the metastable sites, the oxygen seems physisorbed. Each of the Si-O bond lengths is 1.9 Å, much longer than the value of about 1.6 Å in crystalline silica. Compared to the DB site, these are energetically more unfavorable. Furthermore, Miyamoto[8] has simulated the STM images. As for the DB site, the Si atoms originally forming the dimer must be observed as bright spots irrespective of the bias polarity. In the above-mentioned observations, however, any site with this feature has not been identified.

In order to resolve this discrepancy, we investigate the atomic and electronic structures of the oxygen-adsorbed Si(001) surface. For this study, we apply the first-principles molecular-dynamics method. It is based on the local-density-functional formalism with the ultrasoft pseudopotential scheme of Vanderbilt.[9] The implementation of this scheme makes our calculations tractable, because it can largely reduce the energy cutoff of the plane-wave basis set. For this reason, the ultrasoft pseudopotential is successfully applied for various first-principles studies.

In this paper, we find three (meta)stable sites for the atomic oxygen adsorption; the DB site and two different BB sites of dimer atoms. At any sites, the oxygen atoms are chemisorbed to the surface. Most energetically stable is the BB site of the down atom, in opposition to Miyamoto *et al.*[7] Moreover, its characteristic features of the STM images are

compatible to the observed ones of Kliese *et al.*[4]

In the following section, the method of calculation is summarized. The results and discussion are presented in Sec. III. Sec. IV is devoted to a summary.

II. METHOD OF CALCULATION

In this study, we apply the first-principles molecular-dynamics method. It is based on the local-density-functional (LDF) formalism with the ultrasoft pseudopotential scheme of Vanderbilt.[9] The incorporation of this potential[10] makes feasible the calculation for materials including the first-row elements such as the oxygen atom. A plane-wave (PW) basis set is employed to expand the wave functions. For the exchange-correlation interaction, the form of Ceperley and Alder[11] is adopted, which is parametrized by Perdew and Zunger.[12] In order to calculate the atomic forces, we follow the expression of Laasonen *et al.*;[10] the forces are given as negative gradients of the total energy, along with the correction term due to the orthonormality constraints on the wave functions. For tests of the forces, we examine the bulk modulus of the crystal silicon and the vibrational frequency of the oxygen molecule around the equilibrium configurations. Then, the preconditioned conjugate-gradient (CG) method[13,14] is applied to find stable geometries.

First, we construct the ultrasoft pseudopotential of oxygen with the reference configuration of $2s^2 2p^4$. For both the s and p orbital, the cutoff radius is taken to be 1.3 a.u. In order to improve the transferability, two reference energies are set to be the eigenvalues of the orbitals. The other parameters are referred to in Liu *et al.*[15] Because of the softness of this potential, we can get sufficient convergence at the cutoff energy of $E_{\rm cut}=25$ Ry; in all the computations in this work, this cutoff is used. In this way, for the O_2 molecule, the bond length of 1.24 Å and the vibrational frequency of 1450 $\rm cm^{-1}$ are obtained. These values are in good agreement with the experimental ones,[16] although our calculations do not include the spin polarization. They are also comparable to the results of Ref. 10.

Second, the silicon potential is generated in the norm-conserving pseudopotential scheme of Troullier and Martins.[17] The reference configuration is chosen as $3s^2 3p^1$. The cutoff radius for both the s and p orbital is taken to be 1.6 a.u. The sum of the radii of O and Si is a little less than the nearest-neighbor distance between the atoms in crystalline silica of about 3.0 a.u. The potential is transformed to a separable form of Kleinman and Bylander.[18] Then, it gives a lattice constant of 5.38 Å and a bulk modulus of 0.98 Mbar for the diamond silicon. These are in good agreement with the experimental values within an error of 1%.

Lastly, we apply the combination of these potentials for SiO and disiloxane,[19] H_3Si-O-SiH_3, molecules. The Si-O bond lengths in the molecules are obtained as 1.49 Å and 1.62 Å, respectively. The Si-O-Si angle of disiloxane is 144°. These values are in good agreement with the experimental ones[20,21] with an error of about 1%. Moreover, the second derivative of the interatomic potential of the SiO molecule is given as 5.61×10^5 $\rm cm^{-1}$, with an error of a few percent.

In order to simulate the Si(001) surface, we adopt a repeated slab model consisting of eight atomic layers of silicon and a vacuum gap with a thickness of four atomic layers, about 10.3 a.u. The surface unit cell is taken to be $p(2\times1)$. Here, an oxygen atom is placed on each side of the slab to keep the C_2 symmetry. This symmetry keeps the system invariant under the 180° rotation around the appropriate axis parallel to the surface. If we put the oxygen on only one side, it causes fictitious electric field to distort the wave functions.[8] Further, we employ eight **k** points for integrations over the Brillouin zone. Then, we optimize the atomic geometries in the conjugate-gradient (CG) method until the residual force acting on each atom is less than 3.0×10^{-3} hartree/a.u. At the optimization, the two central silicon layers of the slab are fixed at the bulk positions.

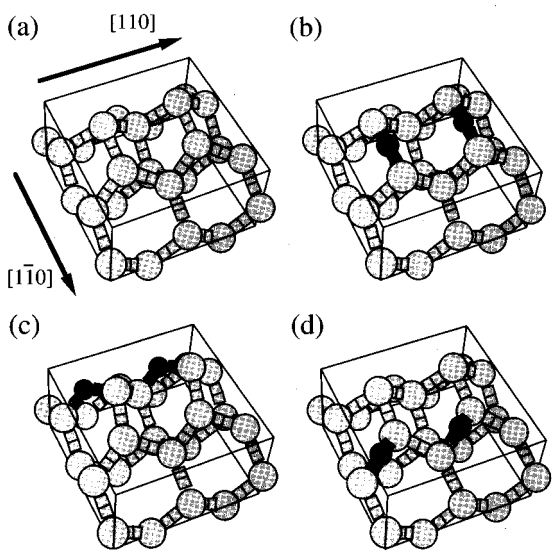

FIG. 1. Perspective views of (a) the Si(001)-2×1 surface and (b), (c), (d) the oxygen-adsorbed surfaces. The oxygen atoms, which are indicated by the closed circles, are adsorbed to the (b) DB, (c) BBu, and (d) BBd sites. In each the view, the unit cell of $p(2\times1)$ is repeatedly depicted. In the figures, the down dimer atoms are in the front, while the up atoms are in the rear.

III. RESULTS AND DISCUSSION

A. Si(001)-2×1 clean surface

First, we determine the stable geometry of the Si(001)-2×1 surface. We find the asymmetric dimer structure with a bond length of $d_{\rm Si\text{-}Si}=2.28$ Å and a buckling angle of $\phi_{\rm Si\text{-}Si}=18.5°$. Its perspective view is shown in Fig. 1(a). These values are in good agreement with the results of the first-principles calculations by Northrup[22] and Ramstad *et al.*:[23] $d_{\rm Si\text{-}Si}=2.29$ Å and $\phi_{\rm Si\text{-}Si}=17.5°$ at $E_{\rm cut}=10$ Ry, and $d_{\rm Si\text{-}Si}=2.26$ Å and $\phi_{\rm Si\text{-}Si}=18.3°$ at $E_{\rm cut}=16$ Ry, respectively. There seems to be a tendency of larger buckling with increasing the cutoff energy. The bond configuration of the down dimer-atom has a strong character of sp^2 hybridization; its three bonds are almost on the same plane. The back-bond is expected to be most strongly stressed in the substrate because it deviates considerably from the tetrahedral configuration around the second-layer atom. For this geometry,

TABLE I. Atomic geometries of the oxygen-adsorbed Si(001) surfaces. For each, the geometry of the adsorption to DB, BB*u*, and BB*d* sites, the Si-O bond lengths $d_{\text{Si-O}}$, the bond angle of the oxygen $\theta_{\text{Si-O-Si}}$, the dimer bond length $d_{\text{Si-Si}}$, and its tilting $\phi_{\text{Si-Si}}$, are tabulated. Here, the tilting of the dimer is represented by the angle between the bond and the $[1\bar{1}0]$ direction. The values of $d_{\text{Si-Si}}$ and $\phi_{\text{Si-Si}}$ before the adsorption are compared. The surface energy (per dimer) relative to that of the BB*d* site is also given.

	DB	BB*u*	BB*d*	Si(001)
$d_{\text{Si-O}}$ (Å)	1.63, 1.63	1.63, 1.67	1.63, 1.69	
$\theta_{\text{Si-O-Si}}$ (deg)	161	124	103	
$d_{\text{Si-Si}}$ (Å)		2.32	2.28	2.28
$\phi_{\text{Si-Si}}$ (deg)		28.0	17.2	18.5
Energy (eV/dimer)	0.12	0.48	0.0	

the energy gain due to the reconstruction is calculated to be 1.62 eV per dimer. This value reasonably agrees with the previous result of 1.7 eV.[24]

In the electronic states, we obtain the surface bands coming from the bonding and antibonding interaction of the dimer, i.e., π and π^* bands. Their energy split at K' point of the Brillouin zone is about 1.3 eV. These bands give characteristic features of the STM images.[25]

B. Atomic geometries of oxygen-adsorbed Si(001) surfaces

Now, we introduce an oxygen atom onto the Si(001) surface. Here, invasion to the inner layers rather than the second one is not taken into account. It is unlikely at the early stage of oxidation. We find three (meta)stable geometries due to the adsorption; the oxygen atom resides at (1) the dimer-bridge (DB) site, (2) the backbond site of the up dimer atom (BB*u*), and (3) the site of the down atom (BB*d*). Perspective views of these structures are shown in Figs. 1(b)–1(d). The Si-O bond lengths $d_{\text{Si-O}}$ and the bond angle of the oxygen $\theta_{\text{Si-O-Si}}$ are summarized in Table I. Those are fairly close to the values in crystalline silica[26] of 1.52∼1.69 Å and 137°∼180°.

At the DB site, the oxygen breaks the original dimer and intervenes between the Si atoms. In contrast, at the BB*u* and BB*d* sites, the dimer is preserved, although it is twisted in the dimer-row direction, i.e., in the [110] direction. The length $d_{\text{Si-Si}}$ and the tilting angle $\phi_{\text{Si-Si}}$ of the dimer bond in each geometry are also summarized in Table I. Here, $\phi_{\text{Si-Si}}$ is defined as the angle between the bond and the [110] direction. The oxygen at the BB*u* site largely lifts up the up atom and displaces it in the [110] direction [see Fig. 1(c)]. At the BB*d* site the dimer bond is retained, almost the same as on the clean surface. The detailed geometry of this adsorption is shown in Fig. 2. Here, we can see that the second-layer atom Si(3) is displaced in the [110] direction. The bond configuration of the down atom Si(1) has a sp^2 character as strong as on the clean surface; Si(1)-O, -Si(2), and -Si(3) bonds are nearly on the same plane. However, the plane is

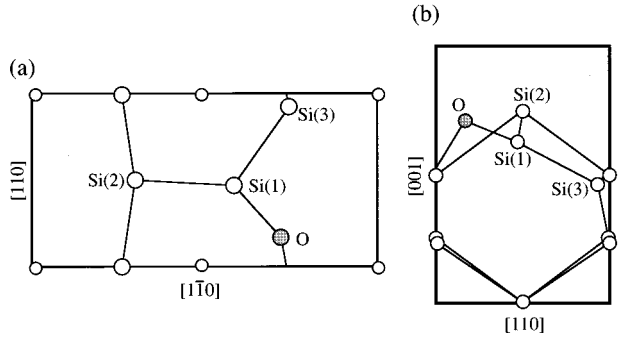

FIG. 2. Detailed atomic geometry of the oxygen adsorption to BB*d* site, projected onto (a) a (001) and (b) a (110) plane. The open and hatched circles indicate the Si and O atoms, respectively. The dimer atoms (1 and 2) and the second-layer one (3) coupled to the down atom are numbered.

slightly rotated around the dimer bond. Then, the up atom is slightly lifted by about 0.1 Å. Moreover, it should be noted that the oxygen breaks one of the mostly stressed backbonds.

Most stable geometry is the adsorption to the BB*d* site. This is a result of the competition among the stress release of the backbond, the energy gain of the dimer bonding, and the stress of the substrate due to the dimer twisting. The DB site is less favorable by 0.12 eV in the surface energy per dimer, as shown in Table I. This stability of the BB*d* site over the DB one is carefully verified by doubling the sample **k** points of the Brillouin zone, by increasing the vacuum thickness of the slab model to six atomic layers, by increasing the cutoff energy to $E_{\text{cut}}=$ 30 Ry, and by extending the unit cell to $p(2\times2)$ for half the oxygen coverage. Further, the BB*u* site is a shallow minimum in the surface energy. It has a fairly large energy of 0.48 eV, compared with the BB*d* site.

In the previous first-principles study,[7] Miyamoto *et al.* have found the DB and BB sites for the adsorption. There is only one BB site, the geometry of which is similar to that of our BB*d* site. At the site, however, the oxygen seems physisorbed to the surface. The Si-O bond length of 1.9 Å is much longer than in crystalline silica. In opposition to us, they have found that the DB site is far more stable than the others. This discrepancy partly comes from their model to simulate the oxygen adsorption; only the oxygen and the Si dimer atoms are relaxed. If all the other Si atoms in the substrate are fixed, the DB site is the most favorable also in the present calculation. Then, the energy difference between the DB and BB*d* sites is about 0.1 eV. This is much smaller than the value in Ref. 7.

C. Electronic structures of oxygen-adsorbed Si(001) surfaces

The oxygen adsorption to the DB site leaves the dangling bonds of the original dimer atoms. Therefore, it gives a metallic character to the surface. This character is clearly shown in the band structure of Fig. 3(a). In contrast, the BB*u* and BB*d* sites are semiconductive. The band structure for the adsorption to BB*d* site is shown in Fig. 3(b). Here, we can see that the surface bands of π and π^* states appear as on the Si(001) clean surface. This is also the case for the adsorption to the BB*u* site. The energy split of these bands at K point of the Brillouin zone is about 1.0 eV and 1.7 eV at

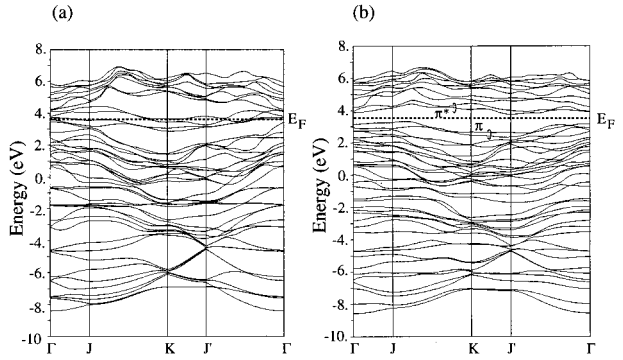

FIG. 3. Band structures of the oxygen-adsorbed Si(001) surfaces to the (a) DB site and (b) BBd site. The Fermi energy E_F is indicated by the dashed line.

the BBu and BBd sites, respectively. These values should be compared to the one of the clean surface (about 1.3 eV). The split width reflects the ionicity of the dimer bond. In the asymmetric dimer, some charge transfers from the down to the up atom.[27] Along with the charge transfer, the width increases from that of the symmetric dimer. Therefore, the above dependence of the energy split on the adsorption site can be easily understood by taking account of the electronegativity of oxygen. The oxygen attracts charge from the bonded Si atoms. Hence, at the BBd (BBu) site, it enhances (reduces) the ionicity of the dimer bond and, in turn, the energy split. This charge transfer at the BBd site has been discussed as affecting the STM images.[8]

As a result of the enhanced ionicity and the slight lift-up of the up atom, the oxygen at the BBd site is expected to give a small protrusion in the filled-states STM images. In the following, it is shown that this is the case. Moreover, the adsorption is much more likely to stabilize local dimer buckling on the Si(001) surface. At room temperature, Wolkow[28] has clarified that the dimers rapidly switch the buckling orientation, leading to an averaged symmetric appearance in STM images. As with atomic defects, the oxygen adsorption probably pins down the nearby dimers into a buckled configuration. However, the adsorption at the DB site is unlikely to do so because of the slight asymmetry. Hence, the expected features at the BBd site are compatible with the observed ones by Kliese *et al.*[4]

Further, we calculate the squared wave functions of the π^* band at K point of the Brillouin zone. In Fig. 4, the plot is given in the $(1\bar{1}0)$ plane through the down dimer atom. Here, we can see that the dangling bond of the down atom is rotated around the dimer bond.

D. STM images

Lastly, we simulate the STM images of the oxygen-adsorbed Si(001) surfaces. Here, the tunneling current between the tip and samples, $I(\mathbf{r},V_S)$, are simply approximated as

$$I(\mathbf{r},V_S) \propto \pm \int_{E_F}^{E_F+eV_S} dE\ \rho(\mathbf{r},E), \tag{1}$$

where the plus (minus) sign is for the positive (negative) surface bias voltage V_S. Further, $\rho(\mathbf{r},E)$ is the local density

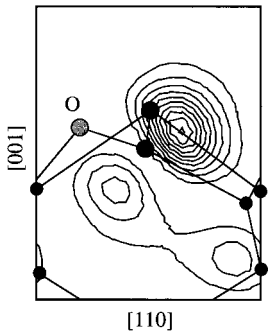

FIG. 4. Contour plot of the squared wave functions of the π^* band for the oxygen-adsorbed Si(001) surface to the BBd site. The plot is given at K point of the Brillouin zone, and in a $(1\bar{1}0)$ plane through the down dimer atom. The contour spacing is 1.0×10^{-3} e/(a.u.)^3. The closed and hatched circles indicate the projected positions of Si and O atoms, respectively.

of states at energy E, and E_F is the Fermi energy. In this approximation, the tip effects of the atomic and electronic structures are ignored.[29]

In Fig. 5, the STM images of the Si(001) surface and the oxygen-adsorbed ones at the DB and BBd sites are given. Here, we plot gray-scale maps of the tunneling current in the logarithmic scale. The scale is settled for each bias polarity, except for the empty-states image at the DB site. The scanning plane of the tip is taken at a height of about 2.2 Å from the surface. This plane is the same in all the slab models for the adsorption. At this height, the images have a good convergence in the qualitative features. Moreover, the bias voltage is taken to be $V_S=-1.0$ V for the filled-states images (the left panels of the figure), or $V_S=+1.0$ V for the empty-states ones (the right panels). The positions of the outermost Si atoms and the oxygen are indicated by the circles with oblique lines and the open ones, respectively.

The STM images of the Si(001) surface are given in Fig. 5(a). The up dimer atom is observed always as a bright spot, while the down one is observed as such only in the empty-

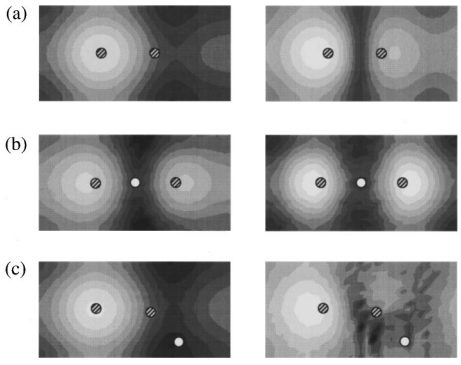

FIG. 5. STM images of (a) the Si(001)-2×1 surface and the oxygen-adsorbed Si(001) surfaces at the (b) DB site and (c) BBd site. The surface bias voltage is taken to be $V_S=-1.0$ V in the left panels and $V_S=+1.0$ V in the right panels. The tip height is set to be 2.2 Å. The gray scale is settled for each bias polarity, except at $V_S=+1.0$ V of the DB site. The horizontal positions of the outermost Si and the O atoms are indicated by the circles with oblique lines and open ones, respectively.

states image. It is less bright than the up atom. This result indicates that the outmost positioning of the up atom gives a dominant effect over the tunneling current. These features of the images agree well with the first-principles results with the atomic-orbital basis set.[25]

The oxygen adsorption drastically changes the images. The STM images of the adsorption to the DB and BB*d* sites are shown in Figs. 5(b) and 5(c), respectively. At the DB site, the original dimer atoms are equally bright irrelevantly to the bias polarity. In the figure, the mirror symmetry with respect to the $(1\bar{1}0)$ plane bisecting the Si-O-Si complex is weakly broken; the brightness of the outermost atoms are slightly different. This is due to the height difference of 0.08 Å in the optimized geometry. The slight asymmetry is unavoidable for any slab model of finite thickness. For this adsorption, the empty-states image is far brighter than the others. This is a result of the metallic character. For this reason, a different gray scale is used for the image in Fig. 5(b). In the experiments,[4–6] any site with these features has not been identified. At the BB*d* site, the filled-states image in Fig. 5(c) closely resembles the one of the clean surface. Here, the up atom gets slightly brighter, as previously expected. In the empty-states image, however, a dull spot is observed in addition to the bright one. This spot comes from the dangling-bond state of the down atom, shown in Fig. 4. In the figure, the mirror symmetry with respect to the (110) plane through the dimer bond is obviously lost. With these features, we can identify the oxygen-adsorbed site on the Si(001) surface. Finally, we should note that the adsorbed oxygen atoms at both the DB and BB*d* sites cannot be directly detected in STM.

IV. SUMMARY

In this study, we have clarified the stable structures of oxygen-adsorbed Si(001) surfaces and their electronic states. Here, the first-principles molecular-dynamics method with the ultrasoft pseudopotential scheme has been applied. We find three (meta)stable sites for the atomic adsorption of DB, BB*u*, and BB*d* sites. Most stable is the geometry of the BB*d* site. The features of its STM images are compatible with the observed ones.[4] Therefore, this adsorption site can be identified in the following way. First, we should find a small protrusion of about 0.1 Å height in the filled-states image. Around this protrusion, local buckling of the dimer row must be stabilized. Second, in the empty-states image, a dull bump beside the protrusion as in Fig. 5(c) should be carefully examined. In the STM image of Ref. 5, we can see several possible sites. We believe that a few of them arise from the oxygen adsorption. For this identification, much more investigation remains to be done. In contrast, the high protrusion with a size of 2×1 unit cell, observed by Kliese *et al.*,[4] might be attributed to the adsorption to the DB site. Its appearance somewhat later than the small protrusions is compatible with the metastability of the DB site.

ACKNOWLEDGMENTS

We are very grateful to Dr. J. Yamauchi and Dr. S. Watanabe for their permission to use their programs of the first-principles molecular dynamics, and kindly support of the computations. One of us (T.U.) thanks Dr. Y. Miyamoto and Dr. H. Kageshima for valuable discussions and comments. Numerical calculations have been carried out at the Computer Center of University of Tokyo. In Fig. 1, we use XMol, version 1.3.1, developed at Minnesota Supercomputer Center, Inc., Minneapolis MN, 1993.

[1] For a good review on the interaction of oxygen and silicon surfaces, see T. Engel, Surf. Sci. Rep. **18**, 91 (1993).
[2] J.A. Schaefer, F. Stucki, D.J. Frankel, W. Göpel, and G.L. Lapeyre, J. Vac. Sci. Technol. B **2**, 359 (1984).
[3] L. Incoccia, A. Balerna, S. Cramm, C. Kunz, F. Senf, and I. Storjohann, Surf. Sci. **189**/**190**, 453 (1987).
[4] P. Kliese, B. Röttger, D. Badt, and H. Neddermeyer, Ultramicrosc. **42**-**44**, 824 (1992).
[5] Ph. Avouris and D.G. Cahill, Ultramicrosc. **42**-**44**, 838 (1992); D.G. Cahill and Ph. Avouris, Appl. Phys. Lett. **60**, 326 (1992).
[6] M. Udagawa *et al.*, Ultramicrosc. **42**-**44**, 946 (1992).
[7] Y. Miyamoto and A. Oshiyama, Phys. Rev. B **41**, 12 680 (1990); Y. Miyamoto, A. Oshiyama, and A. Ishitani, Solid State Commun. **74**, 343 (1990).
[8] Y. Miyamoto, Phys. Rev. B **46**, 12 473 (1992).
[9] D. Vanderbilt, Phys. Rev. B **41**, 7892 (1990).
[10] K. Laasonen, R. Car, C. Lee, and D. Vanderbilt, Phys. Rev. B **43**, 6796 (1991); K. Laasonen, A. Pasquarello, R. Car, C. Lee, and D. Vanderbilt, *ibid.* **47**, 10 142 (1993).
[11] D.M. Ceperley and B.J. Alder, Phys. Rev. Lett. **45**, 566 (1980).
[12] J.P. Perdew and A. Zunger, Phys. Rev. B **23**, 5048 (1981).
[13] M.P. Teter, M.C. Payne, and D.C. Allan, Phys. Rev. B **40**, 12 255 (1989).
[14] D.M. Bylander, L. Kleinman, and S. Lee, Phys. Rev. B **42**, 1394 (1990).
[15] F. Liu, S.H. Garofalini, D. King-Smith, and D. Vanderbilt, Phys. Rev. B **49**, 12 528 (1994).
[16] K.P. Huber and G. Herzberg, *Molecular Spectra and Molecular Structure IV: Constants of Diatomic Molecules* (Van Nostrand Reinhold, New York, 1979).
[17] N. Troullier and J.L. Martins, Phys. Rev. B **43**, 1993 (1991).
[18] L. Kleinman and D.M. Bylander, Phys. Rev. Lett. **48**, 1425 (1982).
[19] We have constructed the ultrasoft potential of hydrogen with the cutoff of 0.8 a.u., following X.-P. Li, D. Vanderbilt, and R.D. King-Smith, Phys. Rev. B **50**, 4637 (1994).
[20] *Numerical Data and Functional Relationships in Science and Technology—Molecular Constants*, edited by K.-H. Hellwege and A.M. Hellwege, Landolt-Börnstein, New Series, Group II, Vol. 14, Pt. a (Springer-Verlag, Berlin, 1982).
[21] *Numerical Data and Functional Relationships in Science and Technology—Structure Data of Free Polyatomic Molecules*, edited by K.-H. Hellwege and A.M. Hellwege, Landolt-Börnstein, New Series, Group II, Vol. 7 (Springer-Verlag, Berlin, 1976).

[22] J.E. Northrup, Phys. Rev. B **47**, 10 032 (1993).
[23] A. Ramstad, G. Brocks, and P.J. Kelly, Phys. Rev. B **51**, 14 504 (1995).
[24] M.T. Yin and M.L. Cohen, Phys. Rev. B **24**, 2303 (1981).
[25] N. Isshiki, H. Kageshima, K. Kobayashi, and M. Tsukada, Ultramicrosc. **42-44**, 109 (1992).
[26] R.W.G. Wyckoff, *Crystal Structures*, 2nd ed. (Interscience, New York, 1965).
[27] D.J. Chadi, Phys. Rev. Lett. **43**, 43 (1979).
[28] R.A. Wlokow, Phys. Rev. Lett. **68**, 2636 (1992).
[29] M. Tsukada, K. Kobayashi, N. Isshiki, and H. Kageshima, Surf. Sci. Rep. **13**, 265 (1991).